

(Submitted to The Physical
Review)

HEPL 558
SLAC-PUB-403

MARCH 1968

1 BEV ELECTRON COMPTON SCATTERING NEAR 180° *

B. Gittelman[†] and W. C. Barber[‡]

Stanford University
Stanford, California

and

W. Selove, D. Tompkins, and F. Forman^{††}

University of Pennsylvania
Philadelphia, Pennsylvania

* Work supported in part by the U. S. Atomic Energy Commission and in part by the U. S. Office of Naval Research Contract [Nonr 225(67)].

[†] Stanford Linear Accelerator Center

[‡] High Energy Physics Laboratory

^{††} NSF Predoctoral Fellow

1 BEV ELECTRON COMPTON SCATTERING NEAR 180°

Abstract

Electrons and positrons near 0° Lab have been measured using bremsstrahlung photon spectra of 950 and 500 Mev maximum energy. The results are interpreted in terms of pair production and electron Compton scattering, the latter contributing primarily for center-of-mass scattering angles near 180° . The results are in agreement with the Klein-Nishina formula to within the accuracy of this experiment, which is about 10%.

Recent experiments^(1, 2) on high energy elastic pion nucleon scattering have demonstrated the existence of a peak in the differential cross section at 180° . One expects a backward peak from a perturbation theory type calculation of a fermion exchange in the crossed channel. However, the experimental peak is much smaller and narrower than might be anticipated from the perturbation calculation. The energy dependence of the magnitude and width of the peak have been

interpreted as evidence for Regge behavior of the fermion propagator⁽³⁾. It seemed interesting to explore the possibility that the attenuation of the backward peak is a general property of the fermion propagator in the crossed channel, not just connected with strong interactions. A comparable situation in quantum electrodynamics is provided by the Compton effect. The Klein-Nishina cross-section⁽⁴⁾ shows a strong peak at 180° CM when the CM energy is much greater than the electron rest mass. This peak comes from the proximity of the fermion propagator to the pole at $u = +m_e^2$ in the crossed channel for scattering angles near 180° (see Figure 1).

Figure 2 shows the center of mass differential cross-section for an incident laboratory photon energy of 1 BeV. The backward peak contains a substantial fraction of the total Compton cross section. Consequently, a useful experimental check of the theoretical value of the height and width of the peak can be made by measuring the integral under the peak, without trying to delineate the peak in detail. With this goal, we have measured the Compton cross section for forward electrons, using bremsstrahlung beams of maximum energy 950 Mev and 500 Mev.

It should be noted that this measurement corresponds to a test of QED theory for a process in which the cross-section is dominated by the pole term $1/(u - m_e^2)$ associated with the virtual electron in Figure 1. We should remark that no deviation

from the theory is to be expected, in view of the recent results of an experiment on electron \rightarrow photons \rightarrow pairs, in the Bev range, involving also similar diagrams with virtual electrons near the pole⁽⁵⁾. Nevertheless, the measurement reported here involves purely electrons and photons, and is one of the most elementary "pure QED" processes possible, and the measurement was therefore worth making.

A preliminary account of this experiment has been given previously, at the International Conference on Electromagnetic Interactions, Dubna, February 1967.

PROCEDURE

The experiment was set up on the 100 inch spectrometer at the Mark III Linear Accelerator at Stanford University. Figure 3 shows a schematic of the experimental geometry. A photon beam was generated by passing an electron beam through $0.0118 \pm .0001$ radiation lengths of radiator (0.0091 radiation lengths of copper plus 0.0027 radiation lengths of aluminum "windows") and then sweeping it out of the way. The photon beam passed through a 10.7 (+0, -0.15) cm liquid hydrogen target and then through a hole in the rear return yoke of the spectrometer magnet. The spectrometer has a rectangular aperture of $(16.5 \pm 0.6) \times 10^{-3}$ radians in the horizontal plane and $(50 \pm 1.3) \times 10^{-3}$ radians in the vertical plane. The inherent momentum resolution of the spectrometer is better than

$\pm 0.3\%$. We used a counter telescope in the focal plane to intercept a momentum bite of $(\Delta P/P) = 0.074 \pm 0.005$.

High energy electrons are produced in hydrogen by the Compton effect and by the pair production process. If we assume the energy spectrum of pair electrons is identical to that of the positrons, then the number of Compton electrons in a particular momentum band is given by the difference between the number of electrons and positrons coming out of the hydrogen in that momentum band. Near the high end of the bremsstrahlung spectrum, the number of Compton electrons is greater than the number of pair electrons, so this is a particularly good place to measure the Compton cross section.

With the incident electron energy fixed at 950 Mev, we took curves of counting rate vs. spectrometer momentum setting for each sign of charge and for full and empty target. The spectrometer momentum was varied from 400 Mev/c to 1 Bev/c. The experiment was repeated with an incident beam energy of 500 Mev. To check that we were observing Compton effect electrons a 0.0091 radiation length copper target was substituted for the hydrogen and the experiment with 950 Mev electrons was repeated. The number of electrons then observed was much closer to the number of positrons, as was to be expected for the higher-Z target. A convenient additional check on the Z-dependence was provided by our empty-target measurements since the front and rear walls of the target

constituted 0.0043 radiation lengths of aluminum. The data from aluminum and copper are consistent with our interpretation of the source of the electrons.

The experiment was run at beam intensity levels between 2×10^5 and 3×10^6 electrons per pulse, with 60 pulses per second of approximately 1 microsecond duration. We used an ionization chamber to monitor the electron beam during the experiment. The ionization chamber was calibrated several times against the laboratory Faraday cup. From the scatter in these calibrations, we estimate the uncertainty in the absolute beam calibration to be $\pm 2.0\%$.

RESULTS AND COMPARISON WITH THEORY

The raw counting rates per initial electron for e^- and e^+ , target full and target empty, are shown in Figure 4 for the 950 Mev run and in Figure 5 for the 500 Mev run. We take the e^+ rates as giving the production of pairs, and the difference between e^- and e^+ rates as giving the production of Compton electrons. Corrections were made for counter dead time (typically 1%) and for counter telescope efficiency (0.986 ± 0.003). The final net rates for pair and Compton electrons are shown in Figure 6, for the 950 Mev run, and in Figure 7 for the 500 Mev run.

In Figures 6 and 7 we also show calculated curves for the expected rates for pair and Compton electrons. These curves

were obtained using the bremsstrahlung spectrum calculated from a computer program of R. Alvarez.⁽⁶⁾ For the Compton effect we used the Klein-Nishina cross section. The curve for pair production was calculated from the papers of Wheeler and Lamb^(7, 8) with the electron contribution corrected according to the prescription of Joseph and Rohrlich.⁽⁹⁾ To be explicit we give the corrected formula in the notation of Wheeler and Lamb (for hydrogen target):

$$d\sigma = \alpha r_o^2 (dE/K^3) \left\{ (E_+^2 + E_-^2) [\Phi_1(\gamma) + \Psi_1(\epsilon) - 4] + (2E_+E_-/3) [\Phi_2(\gamma) + \Psi_2(\epsilon) - 10/3] \right\}$$

where, for hydrogen,

$$\epsilon = \gamma = \frac{100 m_e K}{E_+ E_-}.$$

Ψ_1 , Ψ_2 , Φ_1 and Φ_2 are calculated numerically by Wheeler and Lamb.^(7, 8)

The curves do not include any radiative corrections but do include corrections for the following effects;

1) spread in energy, spatial extension, and angular distribution, for the incident electrons and for the photon beam, and

2) attenuation of photons, and bremsstrahlung, multiple scattering, and annihilation of outgoing electrons and positrons.

We have used the formula of Feynman and Brown⁽¹⁰⁾ to calculate the radiative effects. This formula is not expected

to be accurate for our momentum resolution, but it should be adequate as a basis for an estimate.⁽¹¹⁾ After folding in the continuous photon spectrum and integrating over the spectrometer acceptance we find the correction to the calculated 950 Mev curve is -10%, -7% and -3% at spectrometer settings of 940, 900, and 700 Mev/c, respectively. In view of the smallness of this correction and in view of the magnitude of the systematic uncertainties in our data (beam energy relative to the spectrometer momentum, spectrometer momentum acceptance, beam intensity calibration, and density of liquid in the target) we have not thought it worthwhile to obtain a more sophisticated calculation of all the radiative effects involved in the experiment. We have thus given in Figures (6) and (7) the theoretical curves uncorrected for radiative effects.

Comparing theory and experimental results in Figures (6) and (7) we see that both the pairs and Compton points fit the calculated curves for both energies. The good agreement of the pairs reenforces our confidence that we have understood all the experimental details and is an overall check on the measurement. We finally conclude that the Klein-Nishina formula correctly describes Compton scattering in the region near 180° within our experimental accuracy of $\pm 10\%$.

REFERENCES

- 1) H. Brody et al, Phys. Rev. Letters 16, 828 (1966).
- 2) J. Orear et al, Phys. Rev. 152, 1162 (1966).
- 3) C. B. Chiu and J. D. Stack, Phys. Rev. 153, 1575 (1967).
- 4) O. Klein and Y. Nishina, Z. Physik 52, 853 (1929).
- 5) H. D. Shulz and G. Lutz, DESY, submitted to Berkeley High Energy Conference, Sept., 1966.
- 6) R. Alvarez, Internal report HEPL-228, High Energy Physics Laboratory, Stanford University, July, 1961.
- 7) J. A. Wheeler and W. E. Lamb, Phys. Rev. 55, 858 (1939).
- 8) J. A. Wheeler and W. E. Lamb, Phys. Rev., 101, 1836 (1956).
- 9) J. Joseph and F. Rohrlich, Rev. Mod. Phys. 30, 354 (1958).
- 10) L. M. Brown and R. P. Feynman, Phys. Rev., 85, 231 (1952).
- 11) S. Brodsky (Private Communication).

FIGURE CAPTIONS

Fig. 1. Feynman diagram corresponding to the dominant pole term for 180° Compton scattering. $u \equiv (p' - k)^2$.

Fig. 2. Klein-Nishina cross section for electron Compton scattering at 1 Bev.

Fig. 3. Experimental arrangement.

Fig. 4. Counting rates for e^- and e^+ , 950 Mev run. The ordinate is the number of counts per 1.21×10^8 electrons incident for $\frac{\Delta P}{P} = 0.0742$. The abscissa corresponds to the lower edge of the 7.42% momentum window. Solid curves are for target full; dashed are for target empty.

Fig. 5. Counting rates for e^- and e^+ , 500 Mev run. The ordinate is the number of counts per 1.21×10^8 electrons incident for $\frac{\Delta P}{P} = 0.0742$. The abscissa corresponds to the lower edge of the 7.42% momentum window. Solid curves are for target full; dashed are for target empty.

Fig. 6. Pair and Compton rates, 950 Mev run. The ordinate is the number of counts per 1.21×10^8 electrons for $\frac{\Delta P}{P} = 0.0742$. The solid curve gives the theoretical rates with no radiative corrections included. In addition to the statistical and systematic errors shown, there is an uncertainty in the electron beam energy relative to the spectrometer momentum of $\frac{\delta E}{E} = \pm 0.002$.

Fig. 7. Pair and Compton rates, 500 Mev run. The ordinate is the number of counts per 1.21×10^8 electrons for $\frac{\Delta P}{P} = 0.0742$. The solid curve gives the theoretical rates with no radiative corrections included. In addition to the statistical and systematic errors shown, there is an uncertainty in the electron beam energy relative to the spectrometer momentum of $\frac{\delta E}{E} = \pm 0.002$.

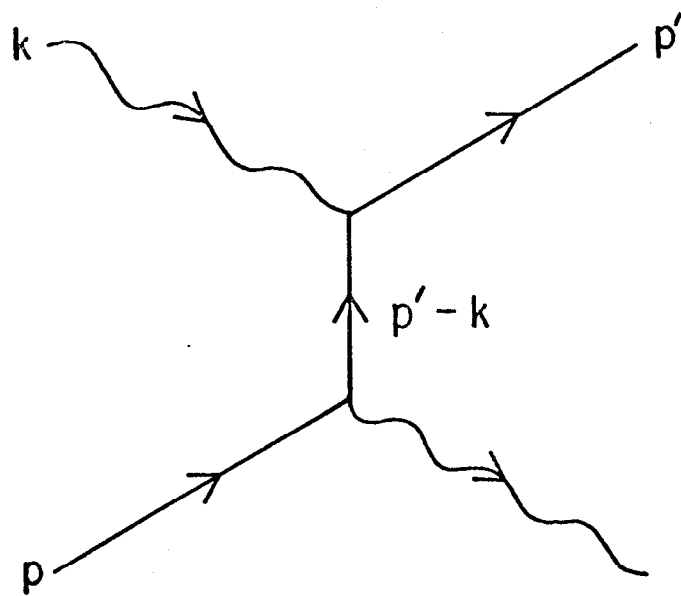


Figure 1

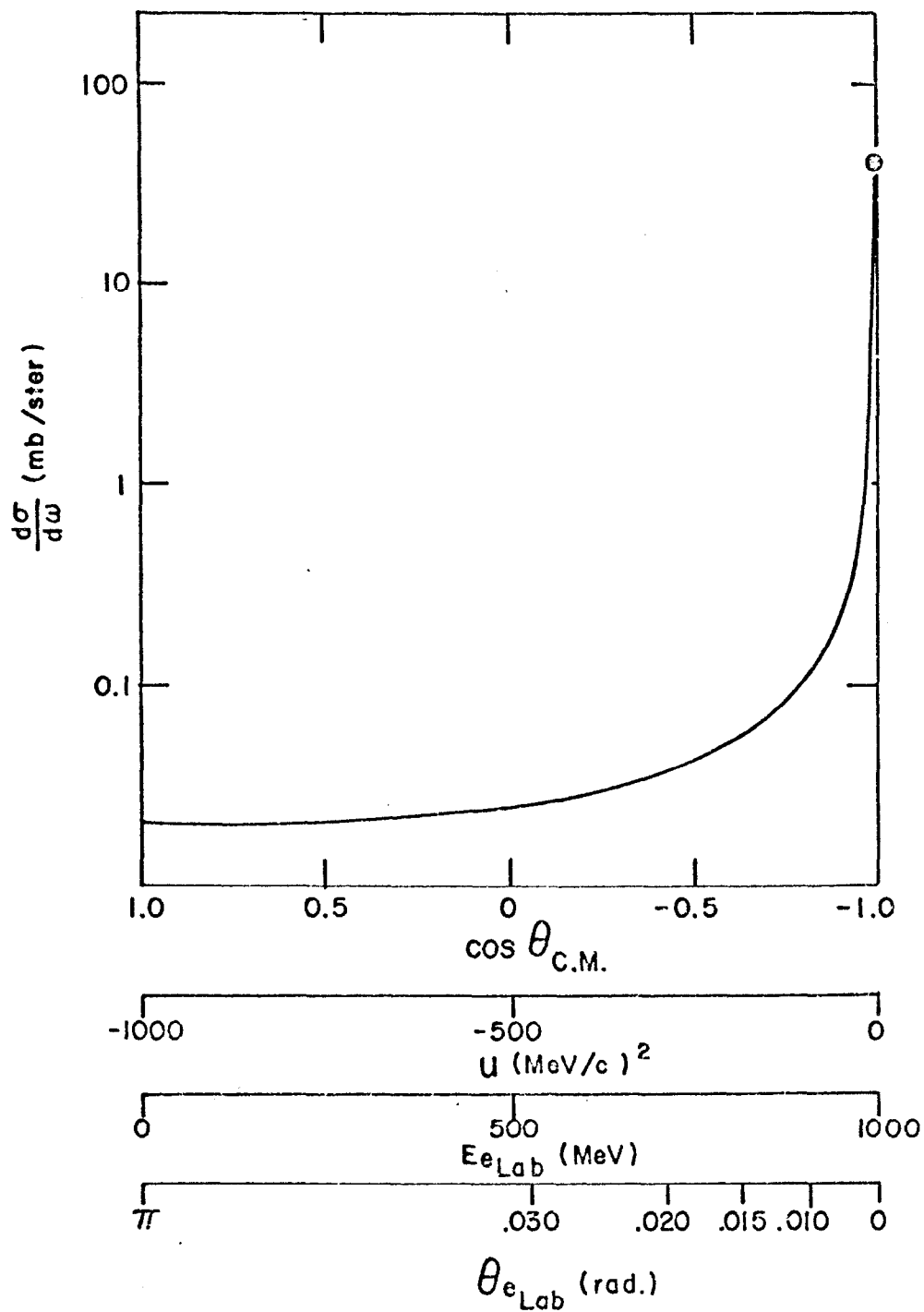


Figure 2

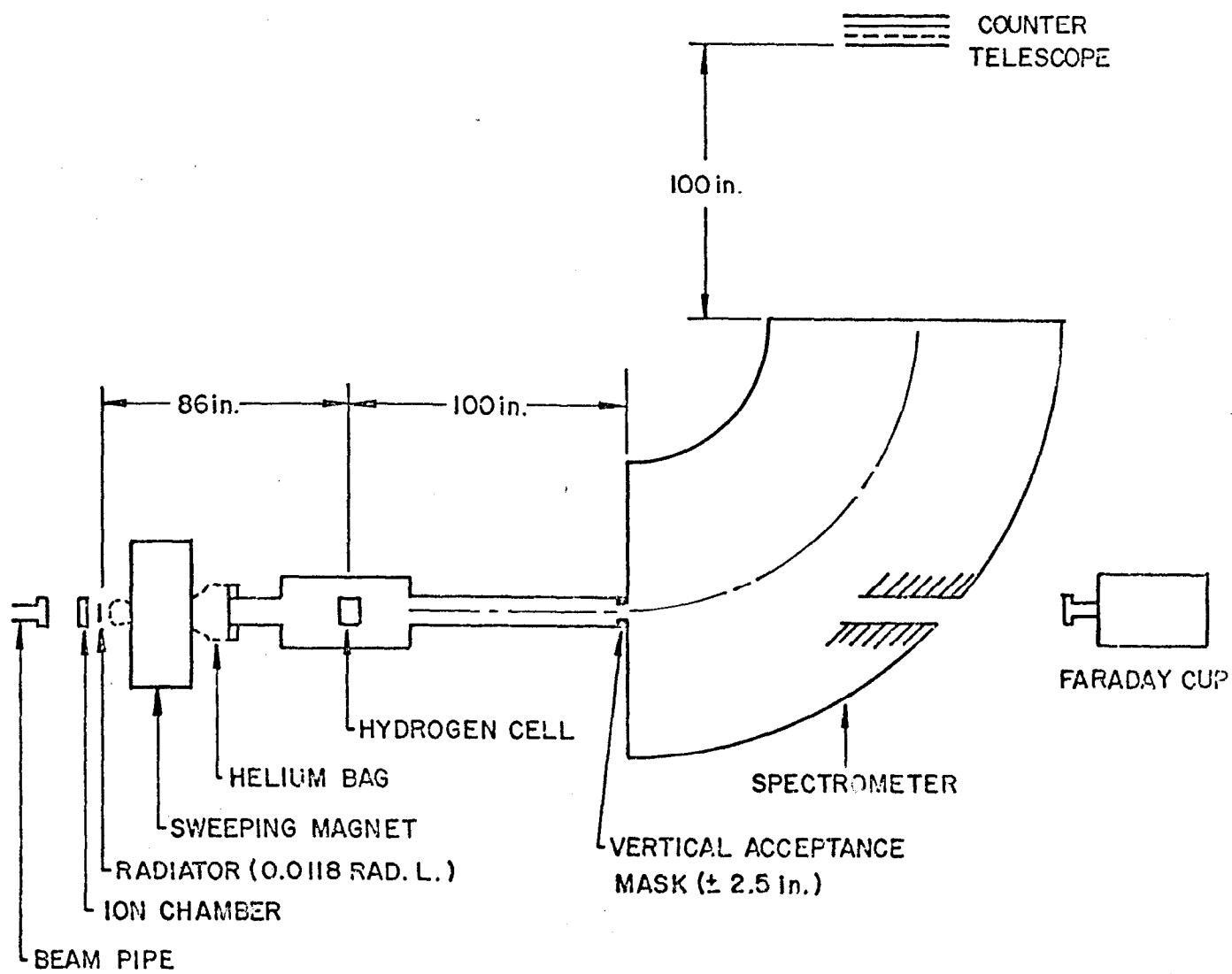


Figure 3

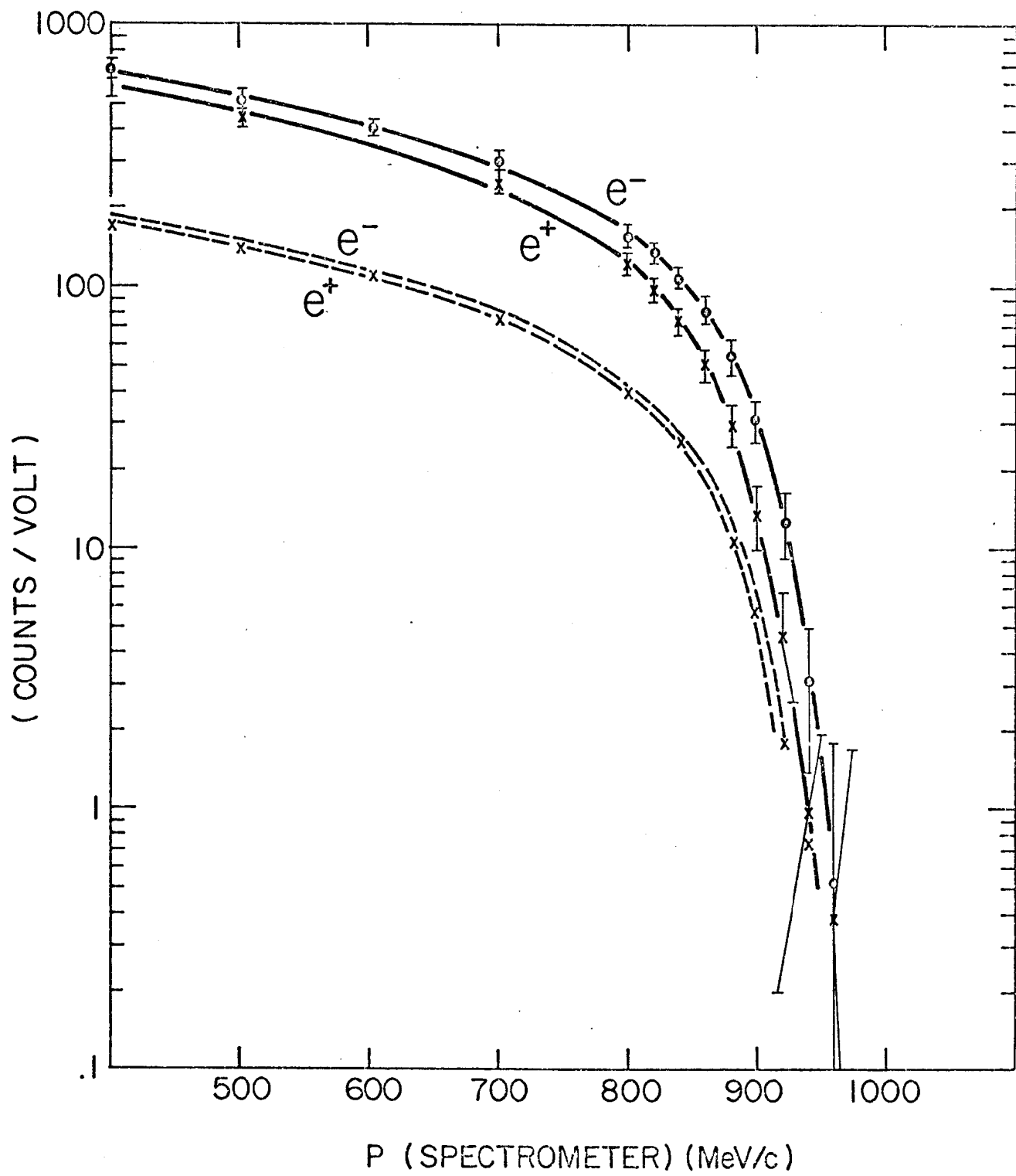


Figure 4

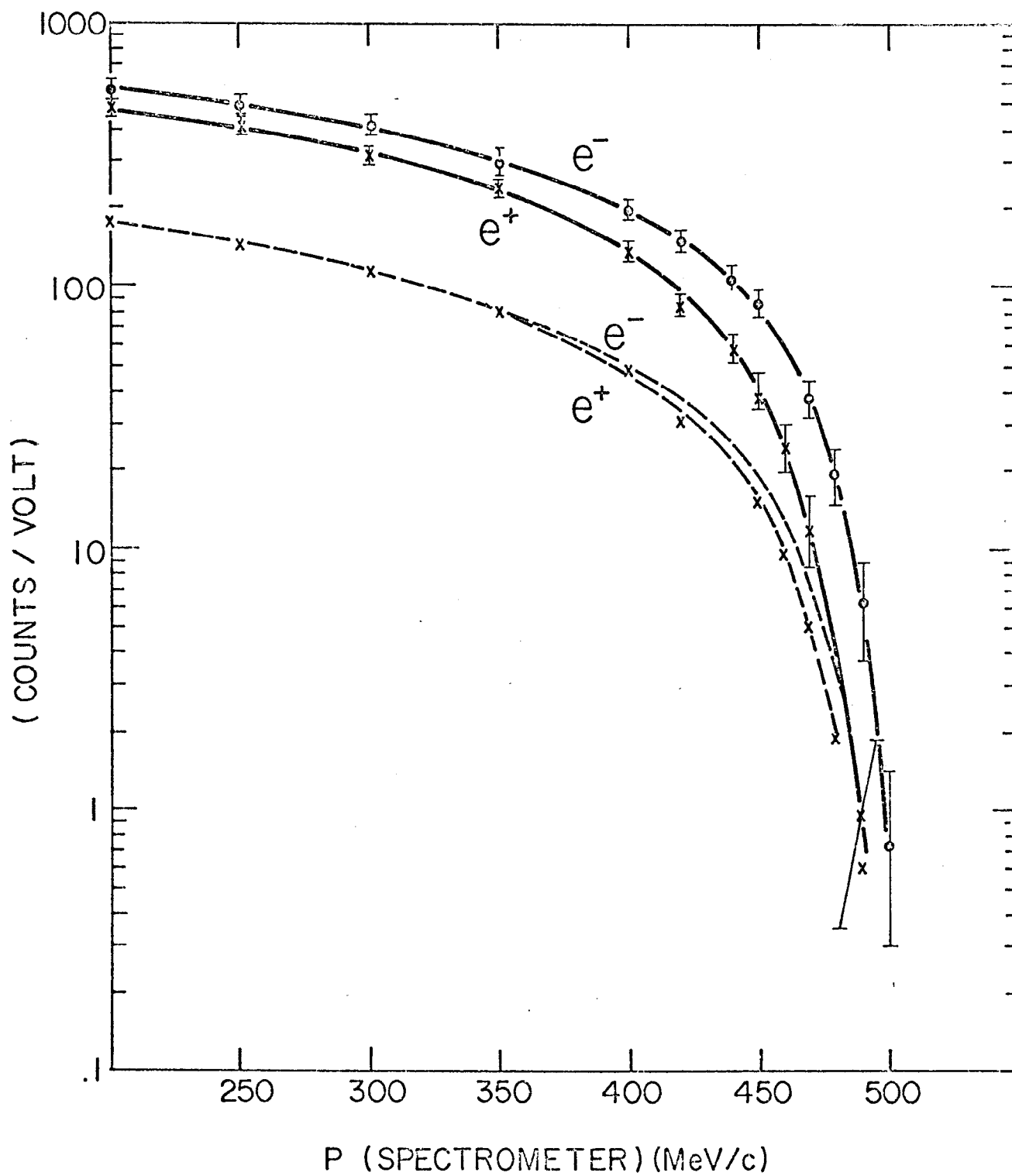


Figure 5

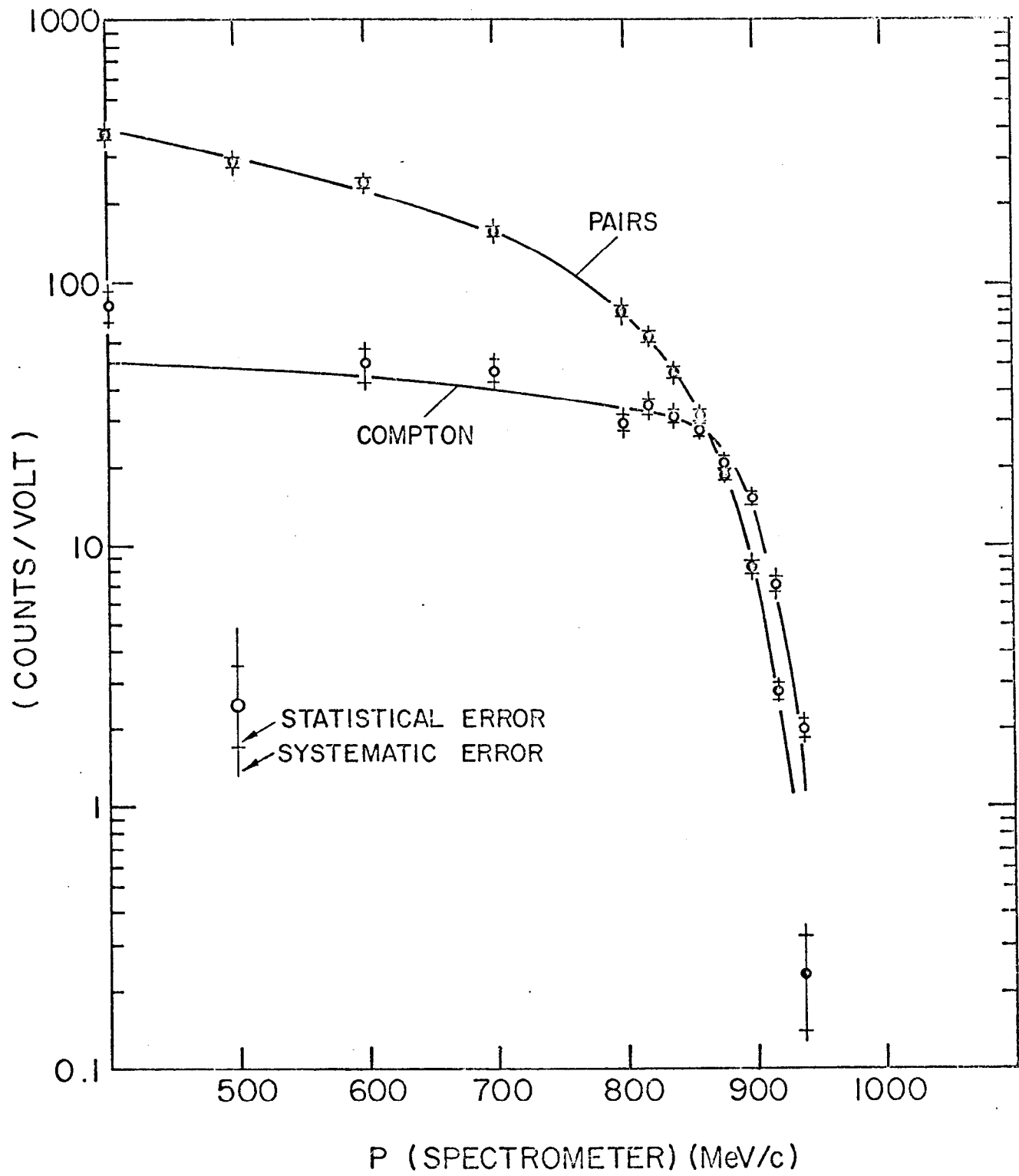


Figure 6

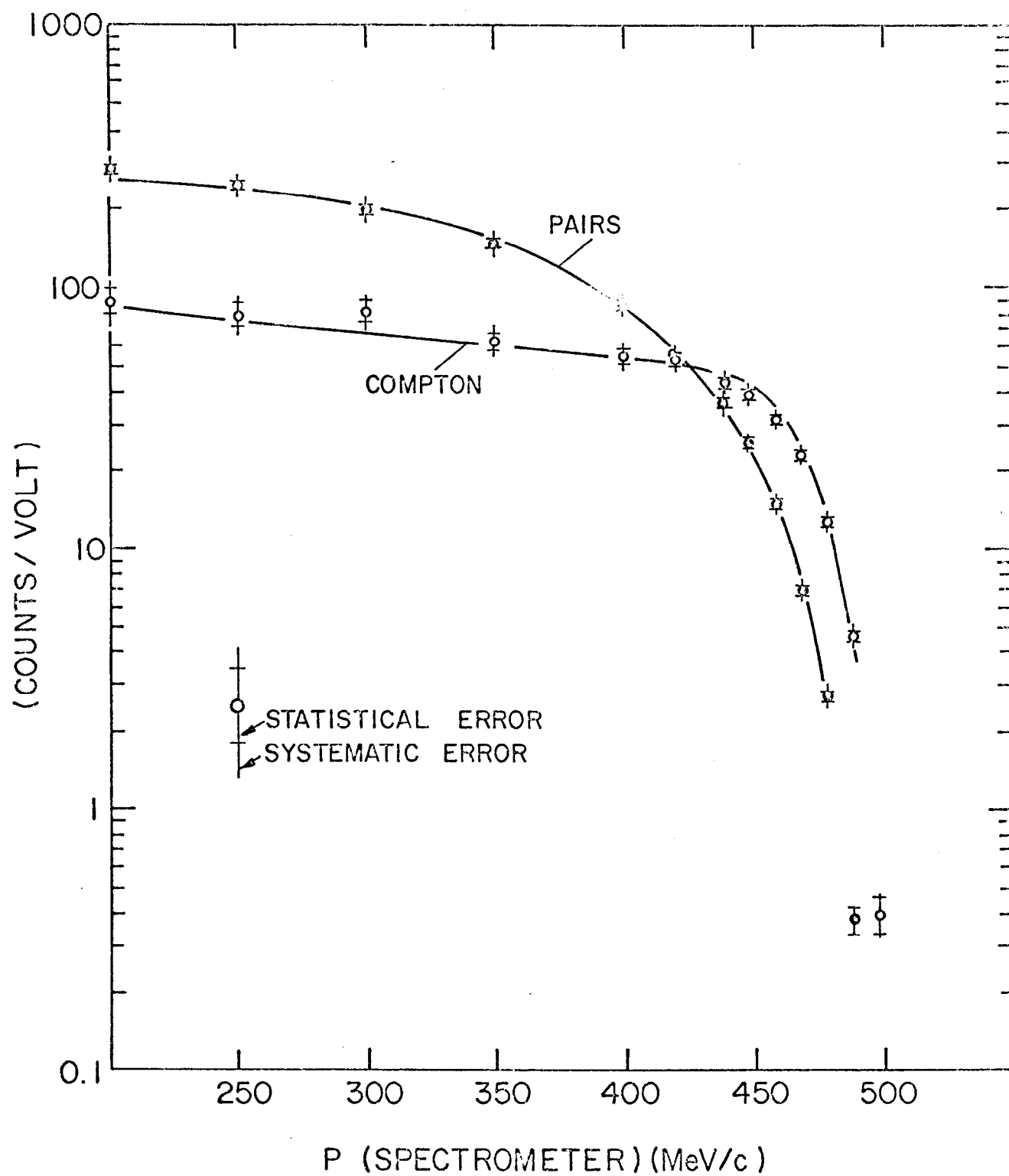


Figure 7